



Determination of lead isotopes in a new Greenland deep ice core at the sub-picogram per gram level by thermal ionization mass spectrometry using an improved decontamination method



Changhee Han^{a,b}, Laurie J. Burn-Nunes^c, Khanghyun Lee^b, Chaewon Chang^{a,b}, Jung-Ho Kang^b, Yeongcheol Han^b, Soon Do Hur^b, Sungmin Hong^{a,*}

^a Department of Ocean Sciences, Inha University, 100 Inha-ro, Nam-gu, Incheon 402-751, Republic of Korea

^b Korea Polar Research Institute, Songdomirearo 26, Yeonsu-gu, Incheon 406-840, Republic of Korea

^c Department of Imaging and Applied Physics, Curtin University of Technology, GPO Box U1987, Perth 6845, Western Australia, Australia

ARTICLE INFO

Article history:

Received 26 December 2014

Received in revised form

2 March 2015

Accepted 3 March 2015

Available online 10 March 2015

Keywords:

Lead isotopes

Greenland deep ice core

Improved decontamination procedure

Silica-gel activator

TIMS

ABSTRACT

An improved decontamination method and ultraclean analytical procedures have been developed to minimize Pb contamination of processed glacial ice cores and to achieve reliable determination of Pb isotopes in North Greenland Eemian Ice Drilling (NEEM) deep ice core sections with concentrations at the sub-picogram per gram level. A PL-7 (Fuso Chemical) silica-gel activator has replaced the previously used colloidal silica activator produced by Merck and has been shown to provide sufficiently enhanced ion beam intensity for Pb isotope analysis for a few tens of picograms of Pb. Considering the quantities of Pb contained in the NEEM Greenland ice core and a sample weight of 10 g used for the analysis, the blank contribution from the sample treatment was observed to be negligible. The decontamination and analysis of the artificial ice cores and selected NEEM Greenland ice core sections confirmed the cleanliness and effectiveness of the overall analytical process.

© 2015 Elsevier B.V. All rights reserved.

1. Introduction

Analytical methods for stable Pb isotopes (^{204}Pb , ^{206}Pb , ^{207}Pb and ^{208}Pb) have proven to be very powerful tools for tracing the provenance of atmospheric Pb, which have also been applied for the analysis of glacial ice [1–4]. However, there are very few reliable measurements of Pb isotopes in the deep polar ice cores, due to extremely low Pb concentrations at or below the picogram per gram level and contaminants being brought to the outside of the core during the drilling operations. Until now, reliable data regarding Pb isotopes from such deep ice cores has been obtained successfully only in a handful of laboratories using thermal ionization mass spectrometry (TIMS) [5–8].

Although ultraclean protocols and techniques for TIMS have previously been established [9,10], the accurate measurement of Pb isotopes at ultralow Pb levels remains an analytical challenge for individual laboratories. This is because it is tremendously difficult to achieve the application of identical laboratory procedures and to ensure minimal analyte contamination. Another problem is the necessity of a stable and enhanced Pb ion beam intensity that

is very important to improve both the reproducibility and the reliability of an isotope ratio measurement on a small polar sample size (tens of pg Pb). Since Akishin et al. [11] used a silica–zirconia gel as an ionization activator for thermal ionization of Pb isotopes in TIMS analysis, the silica-gel activator method using different silica-gels has been widely used in various research areas [12]. Until now, two different silica-gel products were used to determine Pb isotopes in polar snow and ice. The first product is a silica-gel prepared by distilling AR grade silicon tetrachloride (SiCl_4 ; BDH Chemicals) into high-purity water [9], however, the primary drawback of the SiCl_4 is its high reactivity during the reaction, making it difficult to handle. Therefore, it is not easy to produce silica-gel activator with constantly high ion yield efficiency [13]. The second product is a silica-gel produced from the colloidal silicic acid solution (Merck Art. no. 12475) [10,14], however, this product is no longer available commercially. To replace the Merck colloidal silica, Miyazaki et al. [13] evaluated silica-gel activators synthesized using different silica-gels and found that the silica-gel activator synthesized by a silicic acid colloidal solution (PL-7) with a particle size of 0.122 μm and concentration of 23.2% from the Fuso Chemical Co., Ltd., is the optimal silica-gel activator for Pb isotope analysis using TIMS. However, they examined the efficiency of the silica-gel activator by loading samples with 100 ng of NIST (National Institute of Science and Technology, Washington,

* Corresponding author. Tel.: +82 32 860 7708.

E-mail address: smhong@inha.ac.kr (S. Hong).

DC, USA) SRM 981, which requires verification for samples containing much smaller quantities of Pb comparable to polar samples. Moreover, no data on the blank level for PL-7 was provided from their study.

Herein, we report a reliable Pb isotope measurement using an improved decontamination method for deep ice core samples and an optimal silica-gel activator for the thermal ionization of Pb isotopes in TIMS analysis. Our ultraclean analytical procedures proved to ensure contamination control and extremely low blank signals, enabling the reliable simultaneous determination of Pb and Ba concentrations and Pb isotopic ratios at or below the picogram per gram level encountered in polar deep ice cores.

2. Experimental

2.1. Clean laboratories

Analysis of the polar ice core samples with extremely low amounts of Pb requires all the analytical procedures to be performed in a clean environment to minimize contamination. Our experiments were carried out in new non-laminar flow class 1000 (US Federal Standard 209D) clean laboratories that were specially designed for ultra-trace analysis at the Korea Polar Research Institute (KOPRI). Critical care for the clean laboratory design was taken to ensure that construction substances neither contained the analytes to be analyzed, nor posed any contamination problems. All custom made items such as tables, shelves, and hoods used in the clean laboratories were made of PVC or high-density polyethylene (HDPE).

Sample preparations and all analytical procedures were performed inside class 10 vertical laminar flow clean booths or on clean benches installed inside the class 1000 laboratories. These were all made of plastic (PVC) and equipped with ultra-low penetration air (ULPA) filters and plastic pumps. The operators always wore full clean-room clothing and low-density polyethylene (LDPE) gloves during experiments.

2.2. Ultrapure reagents

The first priority for the reliable investigation of ultralow Pb concentration and its isotopes in polar samples is the availability of high-purity water used during every step of the analytical process, from the cleaning of lab ware and decontamination apparatus to the final analysis. In our laboratory, two grades of ultrapure water are used: Millipore Milli-Q water (MQW) obtained by coupling a Millipore RO water purification (Model Elix-3) with a Milli-Q system (Millipore Corp., Model Milli-Q Academic) and sub-boiling distilled ultrapure water (SUW) by a sub-boiling distillation system with two high-purity quartz distillation units (Milestone, DuoPUR) using the MQW. The MQW and SUW are produced inside a class 10 clean booth and the final output rate of the SUW is limited to about 500 mL/day. The SUW produced is stored in a 1 L (or 500 mL) LDPE acid-cleaned bottle (see Section 2.4) and used within 2 days of production.

The Pb content of the water was determined by inductively coupled sector field mass spectrometry (ICP-SFMS), after pre-concentration by non-boiling evaporation and acidification to 1% using Merck “Optima” grade ultrapure HNO₃ [15,16]. The MQW and SUW contained ≤ 0.4 and < 0.05 pg Pb g⁻¹, respectively.

We used different purity grades of HNO₃ for cleaning lab ware and decontamination apparatus. For a series of four acid cleaning baths, guaranteed reagent (GR) grade HNO₃ and Merck “Suprapur” HNO₃ were mainly used for the first and second baths, and Fisher “Optima” grade ultrapure HNO₃ was used for the third and fourth baths. Other reagents used for the preparation of the silica-gel activator and analysis are described in next sections.

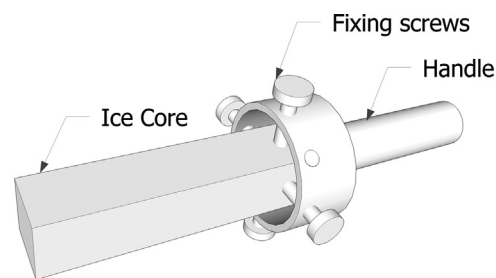


Fig. 1. Schematic drawing of ice core holder for decontamination.

2.3. Selection of laboratory materials

The material and quality of all the lab ware, which contain or come in direct contact with ultrapure samples or reagents, are of primary importance because they may introduce contaminants into the samples or provide an active surface onto which the analytes may be absorbed [17]. As previously proved to be the optimal choice [18,19], LDPE sample bottles and containers (volumes ranging from 15 mL to 20 L) fitted with a polypropylene (PP) cap from Nalgene Company, USA, are always preferred to be used at temperatures less than about 60 °C or for diluted acid concentrations, while fluorinated ethylene propylene (FEP) or PFA Teflon material is employed for storage of concentrated acids and high-temperature evaporation of samples because of the lower chemical inertness and thermal stability of LDPE. Polypropylene is used only for the tips (epT.I.P.S.) of Eppendorf micropipettes and custom-made tongs that are used to handle laboratory items during the cleaning procedures (see next section).

Newly designed decontamination apparatus including ice sample holder and screws (Fig. 1) is all made of Teflon. The exceptional items are the stainless steel chisels and ceramic knives used for the decontamination process. The stainless steel chisels were made using a single plate of 2 mm thick stainless steel type 316 L, which are similar to those used by Ng and Patterson [20] and Boutron and Patterson [21] for Pb analysis in polar samples. To test the purity of ceramic material, of which the cleaning procedures are relatively simpler, commercially available ceramic knives (Kyocera Advanced Ceramics, Models: FK075WH) were also used.

2.4. Cleaning lab ware

Rigorous cleaning of lab ware is critical for controlling contamination levels. The cleaning procedures were originally adopted and slightly modified from the methods as given in detail elsewhere [16,19,22].

In brief, new LDPE lab ware is first degreased with chloroform, rinsed with MQW whilst being held with custom-made PP tongs, and then immersed for a week in the first acid bath (25% GR grade HNO₃ diluted in ultrapure MQW) at room temperature. After rinsing with MQW, we sequentially transfer them into three successive acid baths heated on hotplates at about 40 °C: the second acid bath (25% Merck “Suprapur” grade HNO₃ diluted in MQW) and the subsequent two acid baths (0.2% Fisher “Optima” grade ultrapure HNO₃ diluted in MQW). The items remain immersed in each acid bath for a week. The LDPE bottles and containers taken out from the fourth acid bath are finally rinsed with MQW, filled with 0.1% Fisher “Optima” grade MQW, capped, and stored in sealed, acid-washed polyethylene bags until use. For FEP and PFA Teflon lab ware, they are first immersed in concentrated Merck “Suprapur” HNO₃ at room temperature for at least a week. The subsequent cleaning procedure is the same as LDPE items. PFA beakers used for the preconcentration of the samples by non-boiling evaporation are kept immersed in the fourth acid bath until use.

The initial cleaning procedure for stainless steel chisels involves degreasing with chloroform and immersion in concentrated Merck “Suprapur” HNO_3 for several weeks at room temperature. The chisels are then immersed in each bath of 25% Merck “Suprapur” HNO_3 and 0.2% Fisher “Optima” ultrapure HNO_3 for a week at room temperature. When the chisels are used for decontamination, they are recycled through soaking in concentrated Merck “Suprapur” HNO_3 for 3 h, in 25% Merck “Suprapur” HNO_3 for 3 days, and then left in 0.1% Fisher “Optima” ultrapure HNO_3 until use. Meanwhile, the blade of ceramic knives is degreased with chloroform and then immersed first in 10% AR grade HCl for 24 h, followed by MQW for 24 h. The plastic handles of ceramic knives are covered by parafilm and not immersed in the solutions.

2.5. Improved decontamination method

A key point to obtaining reliable Pb data from polar deep ice cores is to obtain contamination-free deep ice core sections. Until now, the most successful method used to determine Pb isotopes from such ice cores was mechanical decontamination of the outside of the core, using sophisticated ultraclean procedures [5,8,23,24], which were originally developed by Patterson and coworkers at the California Institute of Technology (CIT) [20]. It involved chiseling of successive veneer layers of ice in progression from the contaminated outside to the innermost part in order to obtain the uncontaminated inner part of the core.

Despite high efficiency of the mechanical chiseling method for decontamination of the samples, the main drawbacks of these procedures were that they required two operators and a core length of more than 25 cm, since the core section was required to be fastened with the help of two LDPE tumbler holders with screws [23,25,26]. Apart from the wastage of manpower, the available core length and cross section could be variable, because a full core section obtained as a part of international ice drilling programs is often cut into several parts for various kinds of measurements. For instance, the new NEEM ice core drilled down to a depth of 2540 m during 2008–2012 [27]. For this ice core, only 20-cm long ice core sections with a cross section of $4 \times 4 \text{ cm}^2$ were available for trace element analysis.

To cope with relatively short core length, as well as manpower wastage, we developed a new improved method in a simple way. A given core section was designed to be fastened in the cylindrical homemade Teflon tumblers (5 cm in diameter) using four homemade LDPE screws (Fig. 1). The core section secured parallel to the axis of the tumbler is then decontaminated by chiseling successive layers using ultraclean stainless steel chisels or ceramic knives on a laminar flow class 100 clean bench located inside a cold room at -17°C .

Our new decontamination method was validated using artificial ice cores (AICs) and the NEEM Greenland deep ice core sections. The operator wore full clean-room garb and wrist length LDPE gloves over shoulder length LDPE gloves. The decontamination procedures were as follows. Before starting the process, the visible dirty part from the outside of the core was removed using a stainless steel chisel or ceramic knife, with the core section being kept held. An outermost layer of 1 mm thickness was then first chiseled out parallel to the axis, shaving the edges to make a square core shape slightly rounded. The chips chiseled from the first layer were collected in a specially designed ultraclean LDPE tray laid on a homemade LDPE rack and then transferred into an ultraclean 1 L wide-mouth LDPE bottle. A second layer of 1 mm thickness was subsequently chiseled out using a new chisel and tray, and the chips collected and transferred as previously described. Two successive 1 mm thick layers were then additionally chiseled before reaching the uncontaminated inner part of the core. It is noted that during each round of chiseling successive layers, the exposed end of the core was also chiseled off, but the chips were not recovered. The remaining inner core ($\sim 16 \text{ cm}$ in

length and $\sim 2.8 \text{ cm}$ in diameter) was then recovered directly into an ultraclean 1 L wide mouth LDPE bottle by cutting the end of the inner core of the screwed side with the last stainless steel chisel or ceramic knife. The bottles containing the chips from the successive layers and the inner core were then packed into double sealed acid cleaned LDPE bags and kept frozen until analysis. An aliquot of 10 mL each for Pb, Ba concentrations and Pb isotope analysis was taken in 15 mL ultraclean LDPE bottles after melting the samples on a class 10 clean bench at room temperature.

2.6. Preparation of silica-gel activator

To substitute the previously used silica-gel activator from the Merck, we tested a new silica-gel product supplied from the Fuso chemical Co., Ltd., which is a silicic acid colloidal solution (PL-7) with a particle size of $0.122 \mu\text{m}$ and concentration of 23.2%. SUW and phosphoric acid were used without further purification. The procedure for the synthesis of silica-gel was as follows. Into an acid-cleaned 30-mL LDPE bottle filled with 19 g SUW, 0.094 g of PL-7 was added. To reduce the loading time, 0.098 g Merck “Suprapur” grade 85% phosphoric acid (H_3PO_4) and 0.014 g methanol were added.

2.7. Analytical procedures and mass spectrometry

The procedures of sample processing were similar to those described by Vallelonga et al. [10] and Burn et al. [28]. The ice samples were completely melted and an aliquot of 10 g was weighed in an ultraclean 15 mL PFA beaker containing 10 μL of 65% Fisher “Optima” grade ultrapure HNO_3 , 20 μL of 48% Merck “Ultrapur” grade HF, 4 μL of dilute Merck “Suprapur” grade H_3PO_4 (approximately 5% by weight), and 10 μL of a mixed tracer solution containing accurately known amounts of the enriched isotopes ^{205}Pb and ^{137}Ba . The addition of enriched isotopes enables the quantities of Pb and Ba to be accurately determined by isotope dilution mass spectrometry (IDMS). The sample and tracer mixture were then evaporated to dryness on a Teflon-coated hot plate at $\sim 80^\circ\text{C}$. A droplet of silica-gel activator was then dropped into the evaporated residue and the sample and silica-gel mixture was transferred to a degassed (4 A, 30 min), zone-refined rhenium filament (99.999% Re, 0.7 mm wide, 0.04 mm thick, H. Cross Company). Prior to mounting the sample and silica-gel mixture, the filament was acid cleaned using 7 μL of 1% Fisher “Optima” grade ultrapure HNO_3 at 1.5 A.

Samples were analyzed using a thermal ionization mass spectrometer (TRITON, Thermo Scientific) fitted with a 23 cm radius, 90° magnetic sector containing a 21-sample carousel at KOPRI. All ion beams were measured with a secondary electron multiplier (SEM) operating in ion counting mode. Isotopic ratio determinations were based on more than 10 blocks of measurements, of which each block consists of 10 cycles. The sample and silica-gel mixture loaded on the filament were first dried with a small filament current that was then slowly increased to 1.0 A (700°C) and maintained at this level for 2 min. The current was then increased up to 2.0 A (1200°C) with an increment of 0.2 A every 30 s. When phosphoric acid was completely fumed away, the current was increased to 2.2 A (1350°C) for 2–3 s and then immediately turned down. Two procedural blanks and two or more reference material samples containing a 30–100 pg of NIST SRM 981 Pb isotopic standard were also analyzed together with each batch of up to ~ 21 samples.

Before the measurements, the filament warmed up at 1.5 A during 30 min (preheating). Samples were simultaneously analyzed for Pb and Ba concentrations using IDMS and Pb isotopic composition at 2.0–2.2 A (1200 – 1350°C) [28,29]. The final isotopic ratios were obtained after correction for the blanks. The bias introduced into the isotopic ratios by evaporation of the samples

and other unknown factors was determined by repeated measurements of the NIST SRM 981.

3. Results and discussion

3.1. Ionization efficiency of PL-7 silica-gel activator

Constantly high ionization efficiency of the silica-gel activator is required to determine Pb isotopes in polar samples at the ultralow concentrations. Therefore, we have examined the ionization efficiency of the PL-7 silica-gel activator (SG-PL7) compared to the silica-gel activator (SG-MK) prepared with a colloidal silicic acid from Merck, which was previously used for Pb isotope analysis in polar samples [10]. The ion beam intensity of ^{208}Pb was determined using a 60 pg of NIST SRM 981 reference material and 3 μL of each silica-gel activator. A charged ion beam was generated by preheating (to $\sim 950^\circ\text{C}$) the TIMS filament assembly containing the reference material/Si-gel activator mixture. This was followed by beam adjustment and 300 repeated measurements, with a total integration time of 60 min (10 min filament heating/beam adjustment, 50 min measurement).

Fig. 2 shows the relationship between the elapsed time of measurement and the ion beam intensity of ^{208}Pb for both silica-gel activators. The ion beam intensity of ^{208}Pb using SG-PL7 reached 120,000 counts per second (CPS) after preheating and then shows an exponential decrease (Fig. 2b). However, the ion beam current remained above 40,000 CPS over the course of about 50 min. In

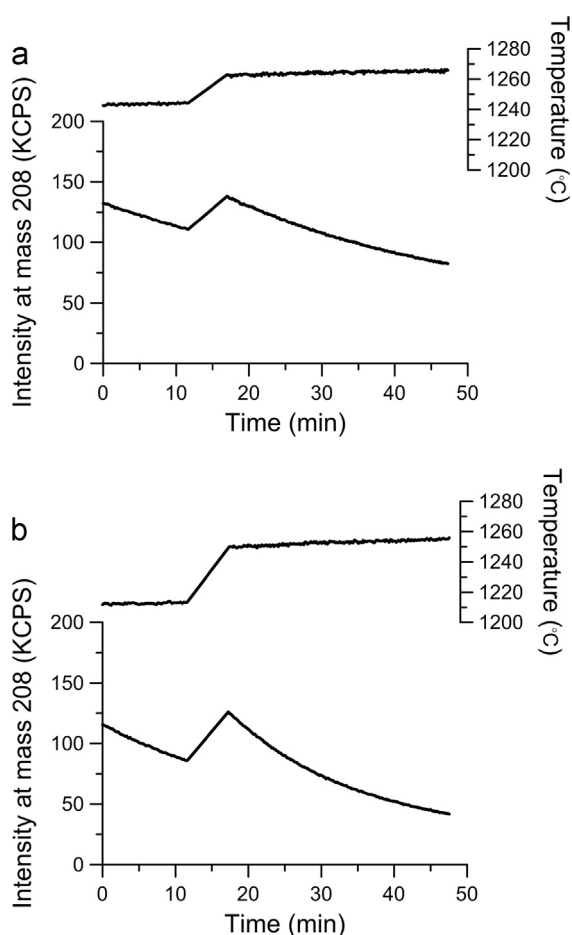


Fig. 2. Ion beam intensity of mass 208 vs. time for a sample of 60 pg NIST SRM 981 for (a) 3 μL of the SG-MK Si-gel activator and (b) 3 μL of SG-PL7 Si-gel activator.

comparison, a higher ion beam intensity (140,000 CPS) was observed for SG-MK with similar signal decay (Fig. 2a). Despite the difference in ion yields between individual silica-gel activators, it is suggested that SG-PL7 could be used as an alternative silica-gel, instead of SG-MK, for synthesizing a new silica-gel activator, to achieve an acceptable level of sufficiently enhanced ion beam intensity for Pb isotope analysis in polar samples containing very small quantities of Pb.

3.2. Mass fractionation

The degree of fractionation, F , is the relative difference (%) per atomic mass unit between the measured NIST SRM 981 and the certified NIST SRM 981, where the measured ratio of isotope i (atomic mass, m_i) to isotope j (atomic mass, m_j) is M_{ij} , and the certified ratio of isotope i to isotope j is S_{ij} , as shown in the following equation [30].

$$F(\%) = \frac{\left(\frac{M_{ij}}{S_{ij}} - 1\right) \times 100}{(m_i - m_j)}$$

And, the associated uncertainty is

$$\partial F(\%) = \frac{\sqrt{\frac{\Delta M_{ij}^2}{S_{ij}^2} + \frac{(M_{ij} \times \Delta S_{ij})^2}{S_{ij}^4}} \times 100}{(m_i - m_j)}$$

In 2009, Burn [30] assumed that fractionation was linearly mass dependent and was calculated using $^{207}\text{Pb}/^{206}\text{Pb}$ ratios, where the $^{206}\text{Pb}/^{206}\text{Pb}$ ratio had an assumed fractionation of 0% per atomic mass unit. Consequently, the final value for fractionation used here is based on the $^{207}\text{Pb}/^{206}\text{Pb}$ ratio. The subsequent fractionation correction factor, f , applied to measured Pb isotopic ratios, is F expressed as a fraction. The final measured Pb isotopic ratios, R_{ij} (and associated uncertainties, ∂R_{ij}), were then determined by correcting measured Pb isotopic ratios and uncertainty for f using following equations [30].

$$R_{ij} = M_{ij} [1 + f(m_i - m_j)]$$

$$\partial R_{ij} = \sqrt{\left(\Delta M_{ij} \times [1 + f(m_i - m_j)]\right)^2 + \left(\Delta f \times [M_{ij}(m_i - m_j)]\right)^2}$$

The final fractionation factor was obtained from the analyses of 30–100 pg Pb loads of NIST SRM 981 isotopic reference material (Fig. 3). The calculated final correction amounted to be $0.24 \pm 0.22\%$ per mass unit, based on the $^{207}\text{Pb}/^{206}\text{Pb}$ ratio, and was used to correct all measured isotopic ratios instrumental fractionation.

Isotope fractionation caused by a decrease in the sample during evaporation on the filament can be estimated by the progressive variation of isotopic ratios within a single run [31]. As shown in Fig. 4, no time-dependent isotope fractionation effect was observed during about 50 min of run time of the NIST Pb standard.

3.3. Determination of procedural blanks

Sufficiently low procedural blank levels, accounting for less than 10% of the total Pb amount, are mandatory to ensure accurate measurement of the Pb isotopic composition of ice core samples. The reagent and loading blanks are shown in Table 1. This demonstrates that the total amount of Pb introduced from the reagents is extremely small, as low as previously reported for the measurement of Pb isotopes in polar ice cores [9,10], and accounts for 60% of the averaged total procedural blank (including the spike). The largest blank level is observed for the loading blank (0.131 pg) which

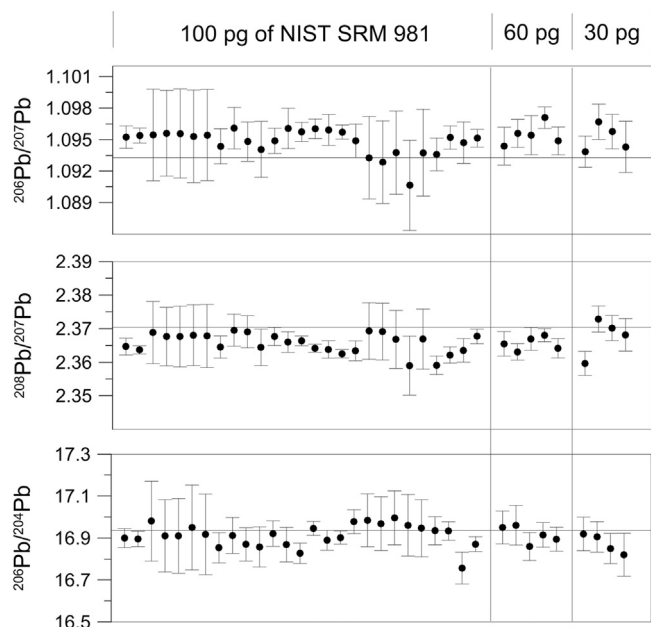


Fig. 3. Measurements of the NIST SRM 981 isotopic standard used to calculate the isotopic fractionation by a decrease in the sample. All ratios have been corrected for isotopic fractionation by $0.24 \pm 0.22\%$ per mass unit using a linear law. These results show a bias of ca. 0.2% for the $^{207}\text{Pb}/^{206}\text{Pb}$ ratio. The error bars indicate 95% confidence interval. The horizontal solid lines are certified values of the NIST SRM 981.

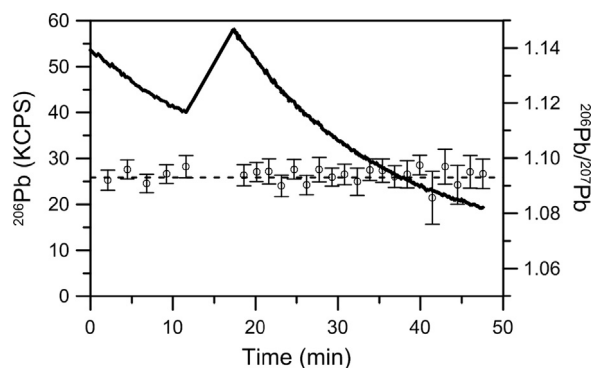


Fig. 4. Relationship among time, ion beam intensity of ^{206}Pb (solid line) and $^{208}\text{Pb}/^{207}\text{Pb}$ ratio (open circle). Dotted line is a certified value of the NIST SRM 981 (1.093). The vertical bars with open circles show the 95% confidence interval of each block (10 cycles).

Table 1
Blank concentrations for individual reagents and ^{205}Pb spike, and loading blanks.

| | Usage (μL) | Pb blank (pg) | Ba blank (pg) | $^{206}\text{Pb}/^{207}\text{Pb}$ |
|---|-------------------------|--------------------|---------------|-----------------------------------|
| Reagent | | | | |
| HNO_3 (ultrapure) | 10 | 0.010 | 0.069 | 1.536 |
| HF | 20 | 0.035 | 0.174 | 1.612 |
| H_3PO_4 | 4 | 0.004 ^a | 0.063 | 1.263 |
| PL-7 silica-gel activator ^b | 3 | 0.045 | 1.305 | 1.026 |
| Natural Pb in the ^{205}Pb spike | 10 | 0.011 | | 1.135 |
| Loading blank ^c | | 0.131 | 1.483 | 0.983 |

^a 5% dilution with SUW.

^b PL-7 silica-gel, phosphoric acid and methanol mixture.

^c PL-7 silica-gel activator, ^{205}Pb spike and Re filament substrate were included.

accounts for $\sim 40\%$ of the averaged total procedural blank (Table A1). The PL-7 silica-gel activator is the primary source of contamination for Ba (Table 1).

Initial procedural blanks were observed to be very high at 18 pg and 15 pg for Pb and Ba, respectively. In order to examine the sources of Pb and Ba contributions added to procedural blanks from air particulate matter and the various containers, we first measured the particle concentrations in the clean bench and clean booth were measured using a portable laser particle counter (Met One Instruments Inc., GT-521, USA). Concentrations of particles ($\leq 0.5 \mu\text{m}$ in size) were found to occasionally exceed the standards of typical clean room particle concentrations, consequently the bench and booth were repeatedly cleaned which allowed particle concentrations to drop within the standard. This process lowered the values of the procedural blanks by about four-fold to 4.04 ± 1.02 pg for Pb and 3.88 ± 4.75 pg for Ba (Table A1). To further evaluate sources of contamination contributing to analytical blanks, pre-cleaned PFA beakers filled with Milli-Q ultrapure water were exposed in UPLA-filtered benches for a period of 14 days. The fallout rates were observed to be $0.042 \text{ pg}/\text{cm}^2/\text{day}$ for Pb and $0.011 \text{ pg}/\text{cm}^2/\text{day}$ for Ba on the sample preparation bench for sample preparation and $0.028 \text{ pg}/\text{cm}^2/\text{day}$ for both elements on the filament loading bench, and as such were insignificant.

Final investigations of sources of contamination focused on LDPE reagent bottles and ^{205}Pb PFA storage vial. This revealed contributions arising from LDPE reagent bottles which were subsequently charged to PFA bottles. As shown in Table A1 and Fig. 5, this further decreased the Pb procedural blank contribution 2.10 ± 0.66 pg, on average, while the Ba blank was not reduced. Investigations of the PFA Teflon 15 mL standard vial with conical interior and PFA closure (Savillex, Eden Prairie, USA) containing ^{205}Pb spike surprisingly showed small powders were detected inside the vial, which may have been introduced during the manufacturing process. It is assumed that such powders could not be effectively removed from the vial interior through the cleaning procedures because of the cone shaped interior. Thus the Savillex PFA vials with conical interior were changed to those with a rounded interior lowered the Pb procedural blank to 0.34 ± 0.24 pg on average, and remained relatively constant (Table A1 and Fig. 5). It is noted that no more decrease in Ba contribution was seen despite proper performance of contamination control for the air and beakers, indicating that the blank level of Ba is mostly controlled by contributions from the reagents and filament. During continuous steps to reduce the blank levels, the average isotopic composition of the procedural blank changed from 1.150 ± 0.001 to 1.042 ± 0.048 for $^{206}\text{Pb}/^{207}\text{Pb}$ and from 2.418 ± 0.001 to 2.173 ± 0.098 for $^{208}\text{Pb}/^{207}\text{Pb}$ (Table A1).

Consequently, the observed blank contributions from the sample treatment are shown to be negligible, representing at most about 1.4% for Pb and less than 1% for Ba in the analyzed NEEM ice core samples with very low concentrations of Pb and Ba concentrations of 2.5 pg g^{-1} and 43 pg g^{-1} respectively (assuming an average sample weight of 10 g, as shown in the next section). These results indicate that special care must be given in the sample preparation process to achieve acceptable and reproducible blank levels, which are required to ensure reliable and accurate measurement of Pb isotopes at ultra-trace concentrations when only small volumes of sample are available.

3.4. Evaluation of an improved decontamination method

To obtain fully reliable data from the ice samples, it is essential to determine the procedural blank from the decontamination process. This has been determined here using AICs. Two AICs were prepared by freezing fresh MQW inside 2 L PFA cylinders (Savillex Corporation). The original MQW was also sampled in a 60 mL ultraclean LDPE bottle to analyze the composition of the water. Before processing the AICs they were cut into the square pillars ($4 \times 4 \times 20 \text{ cm}^3$), to make the core section shape similar to that of NEEM ice cores to be decontaminated, using a band saw machine.

Each cut AIC was mechanically decontaminated as described in Section 2.5, using stainless chisels and ceramic knives separately. Three successive veneer layers were chiseled away before reaching the inner part of the AICs. This procedure allowed evaluation of the level of contamination introduced to each veneer layer and the inner core.

The results of AICs decontaminations are shown in Table 2 and Fig. 6. The concentration and Pb isotopic composition were corrected for procedural blanks contributed from the sample treatment, as described in the previous section. As shown in Table 2, Pb and Ba concentrations are found to be high in the 1st veneer layers of both AICs due to the external contamination. A subsequent decrease is observed by two orders of magnitude in the 2nd layer, confirming the effective removal of the external contamination. Compared with Pb and Ba concentrations in the original MQW, the concentrations measured in the 3rd layer and inner cores exhibit negligible differences for both Pb and Ba (Table 2 and Fig. 6). This shows that no detectable contributions were introduced due to the decontamination procedures by using either stainless chisels or ceramic knives.

Similarly, the 3rd layer and inner cores show insignificant variations in the $^{206}\text{Pb}/^{207}\text{Pb}$ and $^{208}\text{Pb}/^{207}\text{Pb}$ ratios compared with those in the original MQW, despite very small amounts (less than 5 pg) of Pb being used in the analysis (Table 2). This, as well as clear plateaus of low concentrations, definitively confirms that the contamination present on the outside of the ice core has not

penetrated or been transferred to the central part of the AICs and thus demonstrates the validity of the decontamination methods employed here.

3.5. Analysis of the NEEM ice core samples

To confirm the cleanliness and effectiveness of the whole analytical and the decontamination process, four ice core sections selected from the NEEM Greenland deep ice core were processed and analyzed. The depths of the core sections were chosen in such a way that they were expected to have variable Pb and Ba concentration levels and Pb isotopic ratios, due to differing contributions from anthropogenic and natural sources, or differing climatic conditions [5,7,25,26]. These are as follows: one section at a depth of 126 m, dated ~470 years ago (before the year 2000), corresponding to the Renaissance period, during which anthropogenic contribution was already significant [5,25]; two sections from depths of 1281 and 1314 m, dated to ~8920 and ~9440 years ago respectively within the early Holocene and thus devoid of anthropogenic influence and; one section from a depth of 1523 m, dated to 17,240 years ago, and corresponding to the last glacial period, during which Pb and Ba concentrations were highly elevated [7,26]. It is noted that two sections (depths of 126 and 1314 m) were decontaminated using stainless steel chisels and the other two using ceramic knives.

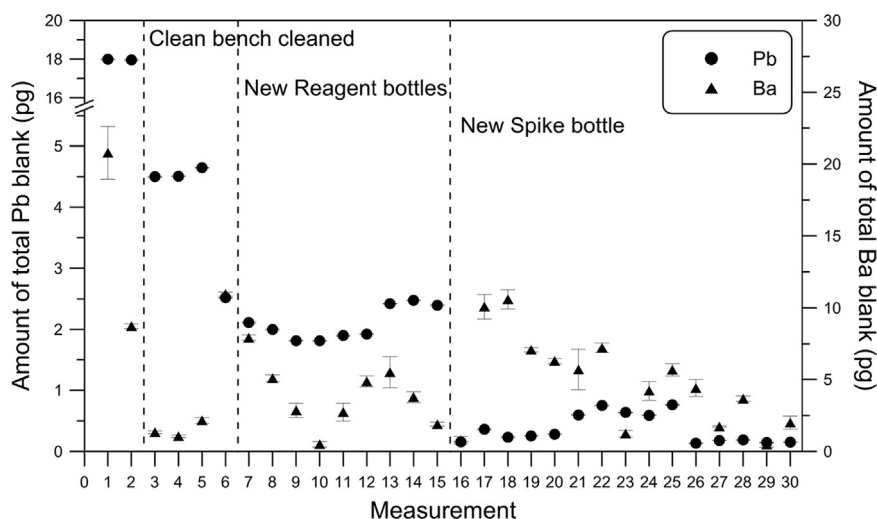


Fig. 5. Measurement of the procedural blank for Pb and Ba contributions from whole sample treatment, all reagents including silica-gel and Re filament substrate. The error bars indicate 95% confidence interval.

Table 2

Results of two artificial ice cores produced by MQW. AIC1 was decontaminated by stainless steel chisels and AIC2 was decontaminated by ceramic knives.

| Veneer | Mass (g) | Concentration | | | | Isotopic ratio | | | |
|----------------|----------|---------------------------|-------|---------------------------|-------|-----------------------------------|-------|-----------------------------------|-------|
| | | Pb (pg g^{-1}) | \pm | Ba (pg g^{-1}) | \pm | $^{206}\text{Pb}/^{207}\text{Pb}$ | \pm | $^{208}\text{Pb}/^{207}\text{Pb}$ | \pm |
| AIC 1 | | | | | | | | | |
| 1st Layer | 9.1 | 173 | 7.4 | 117 | 5.5 | 1.151 | 0.005 | 2.433 | 0.010 |
| 2nd Layer | 9.6 | 1.19 | 0.07 | 4.59 | 0.35 | 1.161 | 0.035 | 2.450 | 0.069 |
| 3rd Layer | 11.2 | 0.31 | 0.03 | 1.11 | 0.17 | 1.168 | 0.056 | 2.461 | 0.108 |
| Inner core | 12.7 | 0.30 | 0.08 | 1.08 | 0.07 | 1.174 | 0.140 | 2.560 | 0.403 |
| Original water | 17.0 | 0.43 | 0.03 | 1.10 | 0.12 | 1.187 | 0.051 | 2.506 | 0.101 |
| AIC 2 | | | | | | | | | |
| 1st Layer | 8.5 | 185 | 7.8 | 49.5 | 5.7 | 1.155 | 0.002 | 2.439 | 0.004 |
| 2nd Layer | 7.6 | 8.47 | 0.46 | 1.54 | 1.12 | 1.148 | 0.002 | 2.431 | 0.004 |
| 3rd Layer | 7.9 | 0.56 | 0.16 | 1.51 | 0.17 | 1.154 | 0.003 | 2.428 | 0.005 |
| Inner core | 9.1 | 0.50 | 0.13 | 1.60 | 0.95 | 1.155 | 0.021 | 2.412 | 0.039 |
| Original water | 12.4 | 0.53 | 0.07 | 1.68 | 0.49 | 1.151 | 0.003 | 2.430 | 0.008 |

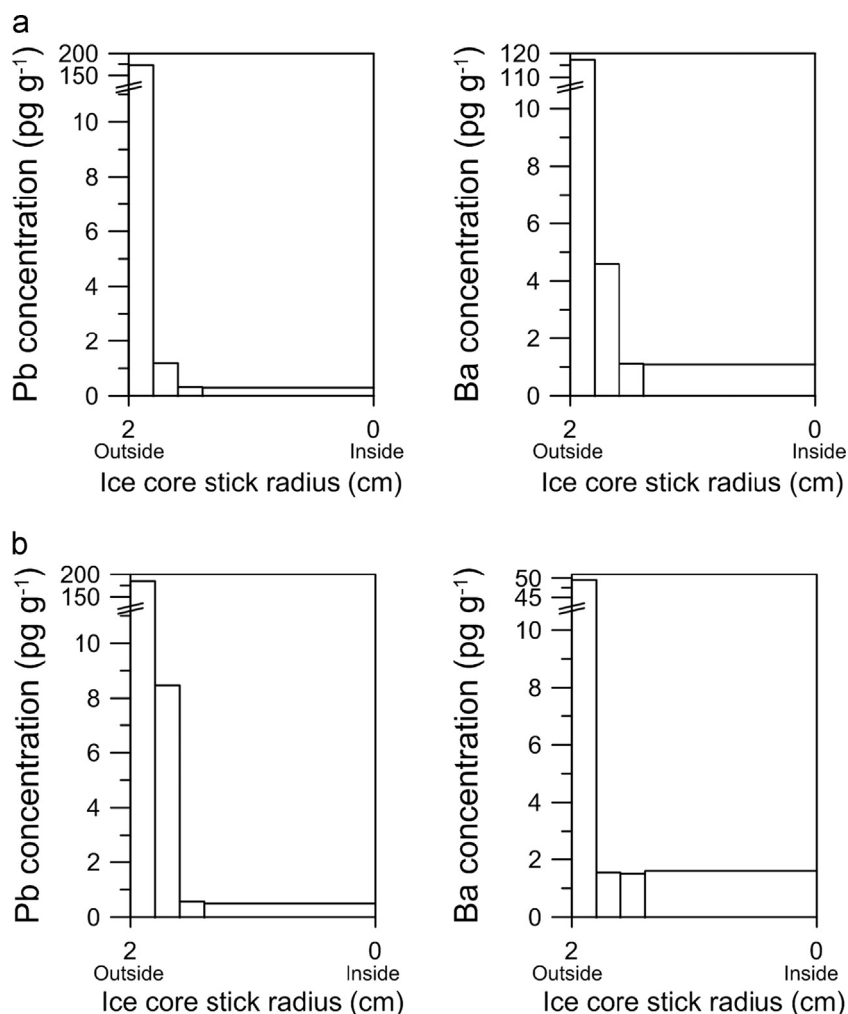


Fig. 6. Decontamination profiles of two artificial ice cores produced by SUW. The former was decontaminated by stainless steel chisels and the latter was decontaminated by ceramic knives.

The outside to inside profiles of concentrations and Pb isotopes in the four sections are shown in Figs. 7 and 8. In all cases, except for Ba in the section at 126 m depth, plateaus of concentrations and isotopic ratios are shown in the inner parts of the sections, indicating that the concentrations and isotopic compositions measured in the inner cores represent pristine values in the ice. Conversely, a continuous decrease of Ba concentrations from the outside to the very center of the core observed for the 126 m depth section indicates that the concentrations obtained in the inner core must be considered as the upper limit of the original concentration in the ice.

Considering detailed features of the profiles, contrasting situations are found for different core sections. Extremely high concentrations up to $\sim 2700 \text{ pg g}^{-1}$ for Pb and $\sim 7800 \text{ pg g}^{-1}$ for Ba were observed in the 1st layer of the 126 m depth section (Fig. 7). On the other hand, the Pb concentration was very low at 14 pg g^{-1} in the outermost layer of the 1281 m depth section, while the Ba concentration was still high ($\sim 1000 \text{ pg g}^{-1}$) (Fig. 8). These features suggest that the outside of the sections is sometimes subject to being highly contaminated for both elements and the contamination is more pronounced for Ba. It is thus proposed that careful precautions must be taken to reduce the outside contamination during the pre-treatment of the core samples when elements to be analyzed are at ultra-low levels. The Pb and Ba concentrations showed a sharp decrease by one or two orders of magnitude in the 2nd layer and then leveled off to well established plateau values in the inner parts

(Figs. 7 and 8), except for the 1523 m depth section corresponding to the last glacial period characterized by much higher concentrations (Fig. 8). Our results conclusively show that the penetration of outside contamination into the inner part was negligible and the decontamination procedures were effective in obtaining contamination-free central parts of the sections.

To verify the reliability of the Pb isotopic ratios observed in the sections, we compared our data with those previously reported from a 3029 m long GRIP ice core from Summit in central Greenland ($72^{\circ}34' \text{ N}$; $37^{\circ}37' \text{ W}$; elevation 3238 m). It is noted that the lower $^{206}\text{Pb}/^{207}\text{Pb}$ signature of the outer layers confirms a different source of Pb in these layers showing extremely high Pb concentrations due to the outside contamination. In the section dated ~ 470 years ago, the $^{206}\text{Pb}/^{207}\text{Pb}$ ratio in the inner core is 1.167 ± 0.004 , which appears to be less radiogenic compared to those observed for the other measured sections (Fig. 7). A less radiogenic $^{206}\text{Pb}/^{207}\text{Pb}$ ratio (1.178 ± 0.001) was also found in GRIP ice dating from 1523 A.D., during which the anthropogenic component was significant [5]. Considering differences in the sample ages and drilling locations between NEEM and GRIP ice cores, the $^{206}\text{Pb}/^{207}\text{Pb}$ ratios in our samples are likely to be in general agreement with that in GRIP ice, representing the isotopic signature of anthropogenic contribution. As for the samples dated ~ 9440 and ~ 8920 years ago, the $^{206}\text{Pb}/^{207}\text{Pb}$ ratios are 1.184 ± 0.013 and 1.201 ± 0.003 , respectively (Figs. 7 and 8). These values are well within the early Holocene $^{206}\text{Pb}/^{207}\text{Pb}$ ratios observed from the GRIP ice core, ranging from

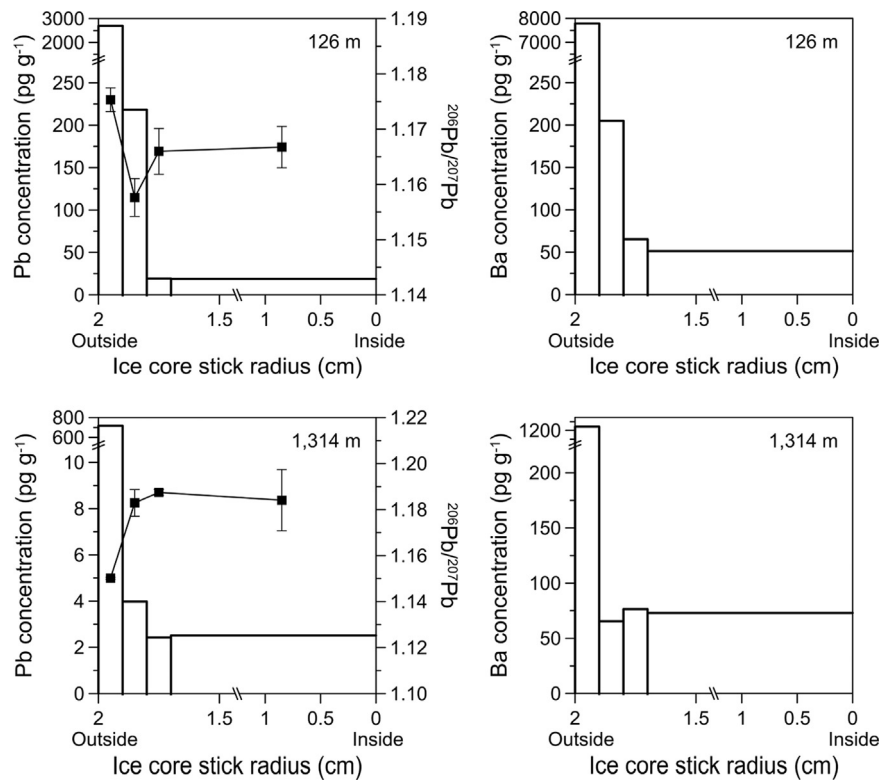


Fig. 7. Decontamination profiles of a 126 m (~470 years ago) and a 1314 m (~9440 years ago) NEEM deep ice core sections from Greenland. These core sections were decontaminated by stainless steel chisels. The error bars of the ²⁰⁶Pb/²⁰⁷Pb isotopic ratios indicate 95% confidence interval.

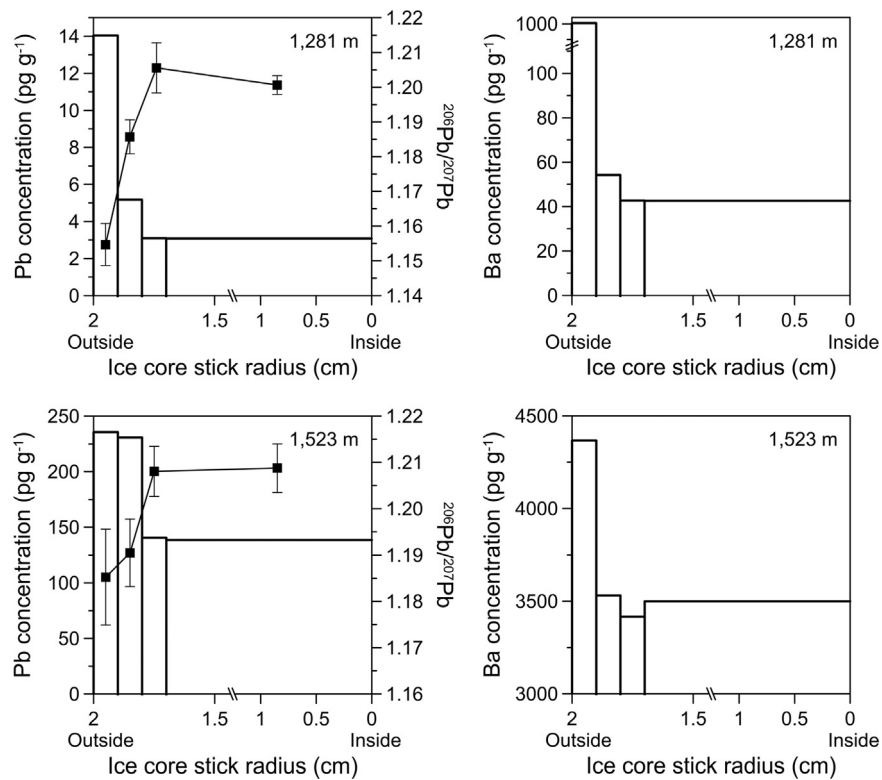


Fig. 8. Decontamination profiles of a 1281 m (~8920 years ago) and a 1523 m (~17,240 years ago) NEEM deep ice core sections from Greenland. These core sections were decontaminated by ceramic knives. The error bars of the ²⁰⁶Pb/²⁰⁷Pb isotopic ratios indicate 95% confidence interval.

1.181 ± 0.010 to 1.202 ± 0.003 between 7295 and 9313 years BP [5,7]. Finally, the ²⁰⁶Pb/²⁰⁷Pb ratio of 1.209 ± 0.005 in the central part of the ice sample dated ~17,240 ago is in good agreement with the ratios (1.210 ± 0.003 – 1.214 ± 0.005) observed in ice dating from

16,960 to 18,949 years BP, corresponding to the last glacial period (Fig. 8). Burton et al. [7] reported that during cooler climatic conditions, the Pb concentrations were mostly attributed to crustal contribution and the isotopic ratios were generally higher when

compared to warmer conditions. Altogether, the profiles of Pb isotopic ratios ensure that isotopic compositions obtained in the central parts of selected NEEM ice core were the original isotopic signature. In addition, they proved that both stainless steel chisels and ceramic knives were useful to produce reliable measurements of Pb isotopes in polar snow and ice.

4. Conclusion

We have presented comprehensive and ultraclean analytical procedures used to determine Pb, Ba and Pb isotopes from polar ice core samples containing picogram amounts using TIMS. A new silica-gel activator produced by PL-7 was validated to show sufficient ionization efficiency for Pb isotope analysis with a very small amount of Pb. When compared with the Pb and Ba contents in Greenland ice, the blank contributions from the sample treatment was found to be negligible. The precision for Pb isotope ratios was estimated to be ~0.28% for a few tens of pg of Pb and no time-dependent isotope fractionation effect was observed.

The cleanliness and effectiveness of an improved decontamination method using either stainless steel chisels or ceramic knives were verified by decontaminating and analyzing the AICs and selected NEEM Greenland ice core sections. The profiles of Pb and Ba concentrations and Pb isotopic ratios suggest that concentrations and isotopic composition in the central parts of selected NEEM ice cores were uncontaminated, representing the pristine values in ice. There is good agreement of the $^{206}\text{Pb}/^{207}\text{Pb}$ ratios between the analyzed NEEM ice samples and previously reported data from GRIP ice core, supporting the reliability of the isotopic measurement.

Finally, our improved decontamination method has allowed the decontamination process to be less manpower-wasteful and time-consuming. The observed cleanliness of ceramic knives makes this material preferable for decontamination because of a simpler cleaning procedure compared to stainless steel chisels. From the outside-inside profiles of concentrations and Pb isotopes, it was found that in order to get the contamination-free central part, at least 2 mm outside of the NEEM ice core sections should be decontaminated before analysis for trace elements.

Acknowledgments

This work was supported in South Korea by the Basic Science Research Program through the National Research Foundation of Korea (NRF) funded by the Ministry of Education, Science and Technology (2012R1A1A2001832). This research was also funded by KOPRI research Grant (PE14010). We wish to thank all personnel involved in the field for the NEEM deep ice core drilling campaign. This work is a contribution to the NEEM project as part of international program supported by funding agencies and institutions in Belgium (FNRS-CFB and FWO), Canada (NRCan/GSC), China (CAS), Denmark (FIST), France (IPEV, CNRS/INSU, CEA and ANR), Germany (AWI), Iceland (Rannls), Japan (NIPR), Korea (KOPRI), Netherlands (NOW/ALW), Sweden (VR), Switzerland (SNF), the UK (NERC), and the USA (US NSF OPP).

Appendix A. Supplementary material

Supplementary data associated with this article can be found in the online version at <http://dx.doi.org/10.1016/j.talanta.2015.03.007>.

References

- [1] K. Rosman, W. Chisholm, C. Boutron, J. Candelone, U. Görlach, *Nature* 362 (1993) 333–335.
- [2] F. Planchon, K. Van de Velde, K. Rosman, E. Wolff, C. Ferrari, C. Boutron, *Geochim. Cosmochim. Acta* 67 (2003) 693–708.
- [3] J. Zheng, W. Shoty, M. Krachler, D.A. Fisher, *Glob. Biogeochem. Cycles* 21 (2007) 1–11.
- [4] K. Lee, S.D. Hur, S. Hou, L.J. Burn-Nunes, S. Hong, C. Barbante, C.F. Boutron, K.J. Rosman, *Sci. Total Environ.* 412 (2011) 194–202.
- [5] K.J. Rosman, W. Chisholm, S. Hong, J. Candelone, C.F. Boutron, *Environ. Sci. Technol.* 31 (1997) 3413–3416.
- [6] A. Matsumoto, T.K. Hinkley, *Earth Planet. Sci. Lett.* 186 (2001) 33–43.
- [7] G.R. Burton, K.J. Rosman, J. Candelone, L.J. Burn, C.F. Boutron, S. Hong, *Earth Planet. Sci. Lett.* 259 (2007) 557–566.
- [8] P. Vallelonga, P. Gabrielli, E. Balliana, A. Wegner, B. Delmonte, C. Turetta, G. Burton, F. Vanhaecke, K. Rosman, S. Hong, *Quat. Sci. Rev.* 29 (2010) 247–255.
- [9] W. Chisholm, K. Rosman, C. Boutron, J. Candelone, S. Hong, *Anal. Chim. Acta* 311 (1995) 141–151.
- [10] P. Vallelonga, K. Van de Velde, J. Candelone, C. Ly, K. Rosman, C. Boutron, V. Morgan, D. Mackey, *Anal. Chim. Acta* 453 (2002) 1–12.
- [11] P. Akishin, O. Nikitin, G. Panchenkov, *Geochemistry* 5 (1957) 500–505.
- [12] M.H. Huyskens, T. Iizuka, Y. Amelin, *J. Anal. At. Spectrom.* 27 (2012) 1439–1446.
- [13] T. Miyazaki, T. Shibata, M. Yoshikawa, T. Sakamoto, K. Iijima, Y. Tatsumi, *Front. Res. Earth Evol.* 2 (2005) 1–5.
- [14] H. Gerstenberger, G. Haase, *Chem. Geol.* 136 (1997) 309–312.
- [15] U. Görlach, C.F. Boutron, *Anal. Chim. Acta* 236 (1990) 391–398.
- [16] S. Hong, A. Lluberas, F. Rodriguez, *Korean J. Polar Res.* 11 (2000) 35–47.
- [17] A.G. Howard, P. Statham, *Inorganic Trace Analysis: Philosophy and Practice*, Wiley, Chichester, UK, 1993.
- [18] C. Patterson, D. Settle, *National Bureau of Standards Special Publication* 422, 1976, pp. 321–351.
- [19] C.F. Boutron, *Fresenius J. Anal. Chem.* 337 (1990) 482–491.
- [20] A. Ng, C. Patterson, *Geochim. Cosmochim. Acta* 45 (1981) 2109–2121.
- [21] C.F. Boutron, C. Paterson, *Nature* 323 (1986) 222–225.
- [22] T. Soyol-Erdene, Y. Huh, S. Hong, H.J. Hwang, S.D. Hur, *Bull. Korean Chem. Soc.* 32 (2011) 2105–2108.
- [23] J. Candelone, S. Hong, C.F. Boutron, *Anal. Chim. Acta* 299 (1994) 9–16.
- [24] K. Van de Velde, P. Vallelonga, J. Candelone, K. Rosman, V. Gaspari, G. Cozzi, C. Barbante, R. Udisti, P. Cescon, C.F. Boutron, *Earth Planet. Sci. Lett.* 232 (2005) 95–108.
- [25] S. Hong, J.P. Candelone, C.C. Patterson, C.F. Boutron, *Science* 265 (1994) 1841–1843.
- [26] S. Hong, J. Candelone, C. Turetta, C.F. Boutron, *Earth Planet. Sci. Lett.* 143 (1996) 233–244.
- [27] D. Dahl-Jensen, M. Albert, A. Aldahan, N. Azuma, D. Balslev-Clausen, M. Baumgartner, A. Berggren, M. Bigler, T. Binder, T. Blunier, *Nature* 493 (2013) 489–494.
- [28] L.J. Burn, K.J. Rosman, J. Candelone, P. Vallelonga, G.R. Burton, A.M. Smith, V.I. Morgan, C. Barbante, S. Hong, C.F. Boutron, *Anal. Chim. Acta* 634 (2009) 228–236.
- [29] S.I. Jimi, K.J. Rosman, S. Hong, J. Candelone, L.J. Burn, C.F. Boutron, *Anal. Bioanal. Chem.* 390 (2008) 495–501.
- [30] L. Burn, *Isotopic and Elemental Tracers in Ice and Snow as Indicators of Source Regions of Aerosols and Changing Environmental Conditions* (Ph.D. thesis), Curtin University of Technology, 2009.
- [31] T. Miyazaki, T. Shibata, M. Yoshikawa, *Proc. Jpn. Acad. Ser. B* 79 (2003) 58–62.